



Log-based rock compressibility estimation for Asmari carbonate formation

Rahman Ashena¹ · Peter Behrenbruch¹ · Ali Ghalambor²

Received: 19 December 2019 / Accepted: 11 June 2020 / Published online: 20 June 2020
© The Author(s) 2020

Abstract

Rock compressibility has many applications in the upstream petroleum industry, for example, reservoir material balance calculations and geomechanics, as related to possible formation compaction and subsidence. When measurements on core are not available, empirical correlations may need to be considered, derived for specific fields. In the study presented, the suitability of the log-based method for evaluating rock compressibility is investigated, with the aim of deriving a suitable correlation for Asmari carbonate, Southwest Iran. A stepwise log-based method of rock compressibility determination is presented, including the construction of a geomechanical earth model, MEM. In comparing a log approach with core-derived results, it was found that the log-based method showed a rather reliable estimation of pore compressibility for carbonates studied, except for intervals with extremely large wellbore washout. Although the selected procedure is similar to that used for sandstone by other researchers, involving in some cases complex procedures, a relatively good matching result could be obtained with a relatively simple procedure. To validate the results from this study, a comparison of compressibility values is made with several industry correlations. An application of formation compressibility for estimating possible formation compaction and associated subsidence is also presented. However, a minimal effect is indicated in this case, as the carbonates studied are rather consolidated. In summary, this study presents a new correlation for rock compressibility for Southwestern Iranian carbonate oilfields (Asmari carbonate), validating the applicability of a log-based technique.

Keywords Rock compressibility · Log-based estimation · Geomechanical approach

Introduction

Rock compressibility is a significant parameter in reservoir studies, for example, material balance as related to estimating (remaining) reserves. Another application involves the prediction of possible formation compaction and associated surface subsidence, a complex geomechanical problem. Rock compressibility has also application in well completions and associated sand control operations (Ghalambor et al. 1994). Core-based compressibility measurements, especially for consolidated rock, are always the first choice. However, when such data are not available, alternative techniques need to be considered.

This study presents an investigation of a cost-effective log-based method of compressibility estimation for Asmari

carbonate formation. The approach is validated by comparison with core-derived measurements. Compressibility results were also used to evaluate the possibility of compaction-related subsidence.

It is common practice by the industry to use published, empirical correlations of rock compressibility, presented at net over-burden pressure, NOBP versus atmospheric porosity, in cases when core measurements are unavailable. Correlations are derived for specific NOBP conditions (reservoirs, fields or regions) and therefore may not be directly applicable for another region. Ideally, correlations should be derived for specific fields, to minimize possible errors. This study fills the gap in considering Iranian, Asmari carbonate formation, as demonstrated by comparison with existing correlations reported in the literature. For each existing industry correlation, deviations for the study dataset were determined, resulting in the identification of the most applicable correlation. The identified correlation can then be deployed for other fields in the region by simply knowing atmospheric porosity.

✉ Rahman Ashena
ashena.rahman@gmail.com

¹ Bear and Brook Consulting, Brisbane, Australia

² Oil Center Research International, Louisiana, USA

A concern is that core compressibility measurements may not always be reliable, specifically as derived from hydrostatic tests. There is also the possibility of invalid, failure-related results from uniaxial testing. The less expensive, log-based technique presented here may prove to be advantageous, especially when the formation being considered is relatively uniform, as is the case for the carbonate formation under consideration. The methodology selected is similar to more standard techniques used for sandstone formations; more complex methods such as those proposed by Saxena (2011) were not considered. Log-based estimates are compared with core-based evaluation, imposing a cutoff to identify unreliable results.

Finally, using the compressibility values derived for the reservoir under consideration, following a rigorous stepwise mathematical description, the compaction-related subsidence for the reservoir is investigated, following decades of production.

Review of rock compressibility definitions and applications

Rock stress and related strain, and their relations have been in use for considerable time. In solid mechanics, for elastic materials, the following relationship holds between strain, ϵ and the effective stress, σ (Hakiki and Shidqi 2018):

$$\epsilon = \frac{1}{E} \sigma \quad (1)$$

where E is Young's modulus of elasticity.

In fluid mechanics, the following relationship holds between shear stress, τ and shear rate (strain), γ :

$$\gamma = \frac{1}{\mu} \tau \quad (2)$$

where μ is fluid viscosity.

For almost all reservoir rocks which are elastically deformable, the relationship between volume and loading is nonlinear (van der Knaap 1959). The coefficient of compressibility has been defined as the strain divided by stress, which is comparable to the reciprocal of Young's modulus in solid mechanics and to the reciprocal of viscosity in fluid mechanics. The coefficient of isothermal compressibility is generally defined as the relative volume change of a material (i.e., strain) per unit change in effective stress under conditions of constant temperature. The compressibility coefficients (which are always positive values) are defined separately for the bulk, rock matrix and pore space as the pore pressure varies (after Zimmerman et al. 1986):

$$C_{bp} = -\frac{1}{V_b} \left(\frac{dV_b}{d(\text{NOBP})} \right)_c \quad (3)$$

$$C_{mp} = -\frac{1}{V_m} \left(\frac{dV_m}{d(\text{NOBP})} \right)_p \quad (4)$$

$$C_{pp} = -\frac{1}{V_p} \left(\frac{dV_p}{d(\text{NOBP})} \right)_p \quad (5)$$

where C_{bp} (or simply C_b) is the coefficient of bulk compressibility as the pore pressure drops [psi^{-1}]; the first subscript denotes the type of compressibility and the second subscript denotes the changing pressure, C_{mp} (or simply C_m) is the matrix compressibility coefficient [psi^{-1}], C_{pp} (or simply C_p) is the pore volume compressibility coefficient [psi^{-1}], V_b , V_m , and V_p are the bulk, matrix and pore space volumes [cm^3], respectively,

The subscript "c" indicates that confining pressure is constant; "p" indicates that the pore pressure is constant.

NOBP is the net over-burden pressure or effective stress [psi].

The net over-burden pressure, NOBP is the effective stress, with the definition first given by Terzaghi (1936), and later modified by Biot (1941) to:

$$\text{NOBP} = \sigma_v - \alpha P_p \quad (6)$$

σ_v is the vertical or overburden stress (psi^{-1}), which can be found from bulk density logs (Ramiah et al. 2019) or from the estimated overburden stress gradient in a region, α is Biot's coefficient [dimensionless], and P_p is pore pressure [psi^{-1}], which is typically measured by repeat formation tester (RFT), modular dynamics testing (MDT), well test analysis, logging while drilling sensor (Ashena et al. 2020), or can be estimated using Dc-exponent or kick data from daily drilling reports (Ashena et al. 2020; Farsimadan et al. 2020).

Comparing different compressibility terms, the following relationship holds between the mentioned compressibility coefficients (Domenico 1977):

$$C_b = \varphi C_p + (1 - \varphi) C_m \quad (7)$$

As C_m is an order of magnitude smaller than C_p , it may be ignored (Laurent et al. 1993):

$$C_m = -\frac{1}{V_m} \frac{dV_m}{d(\text{NOBP})} \approx 0 \quad (8)$$

Combining Eqs. 7 and 8, C_b can be related to C_p by:

$$C_b = \varphi C_p \quad (9)$$

Alternatively, it can be expressed as:

$$C_p = \frac{C_b}{\varphi} \quad (10)$$

Pore volume compressibility, C_p , which is also named rock compressibility C_r , has two main applications in the petroleum industry:

- *Reservoir simulation:*

In any (dynamic) reservoir simulation software, rock compressibility is traditionally required as the only geomechanical input parameter which can have significant effect on the results (Falcao et al. 2015). The effect is included in material balance calculations and the evaluation of original-oil-in-place, especially in under-saturated volumetric reservoirs (i.e., oil reservoirs without any gas caps) and also when the limits of the field are unknown or undefined. In simple simulation models, a single, constant compressibility value is entered for the entire reservoir simulation model. However, using a relationship for compressibility would better represent the formation stress–strain behavior for a particular reservoir situation (Falcao et al. 2015). In any (dynamic) reservoir simulation software, rock compressibility is traditionally required as the only geomechanical input parameter which can have significant effect on the results (Falcao et al. 2015). The effect is included in material balance calculations and the evaluation of original-oil-in-place, especially in under-saturated volumetric reservoirs (i.e., oil reservoirs without any gas caps) and also when the limits of the field are unknown or undefined. In simple simulation models, a single, constant compressibility value is entered for the entire reservoir simulation model. However, using a relationship for compressibility would better represent the formation stress–strain behavior for a particular reservoir situation (Falcao et al. 2015).

- *Compaction and subsidence:*

Having determined pore compressibility, possible formation compaction and associated subsidence at surface can be estimated. Using core and log-based estimates of rock compressibility, this study shows how the magnitude of compaction is estimated for a specific case involving Asmari carbonate. Having determined pore compressibility, possible formation compaction and associated subsidence at surface can be estimated. Using core and log-based estimates of rock compressibility, this study shows how the magnitude of compaction is estimated for a specific case involving Asmari carbonate.

Methods for estimating rock compressibility

There are two methods discussed in this paper to estimate rock compressibility:

Selection of best-matching industry correlation

Core compressibility measurements may be unavailable for a region under study, or the core compressibility test may be technically difficult to execute, produce questionable results or is very costly, e.g., unconsolidated formations. In such cases, published correlations of rock (or pore) compressibility C_r at initial net over-burden-pressure, NOBP_i vs atmospheric porosity, i.e., rock porosity at the surface, is typically used by the industry (Hall 1953; Newman 1973; Khatchikian 1995). Table 1 shows several published correlations for C_r for carbonates as a function of atmospheric porosity. Most of these empirical correlations have been developed only for well-consolidated rock, except for Horne (1990) and modified Horne correlations (Jalal 2006), derived for both, consolidated and unconsolidated sandstone, and also carbonates. For very shallow sandstone formations, containing soil or clay, soil compressibility models should be considered (Santamarina et al. 2019). For consolidated formations, the lower the porosity, the greater the pore compressibility (van der Knaap 1959). However, this trend may be the opposite for friable and unconsolidated formations. Deviation from expected trends, e.g., the modified Horne correlation may be related to other factors such as in situ depth and effective stress, as well as specific rock type; if such factors are ignored compressibility estimates are often in error (Newman 1973).

Generally, to estimate compressibility for a field or region in a cost-effective manner, it is recommended to first take core samples and conduct compressibility laboratory tests in some wells of the field. Next, using the available laboratory data, it is recommended to find the best-matching correlation for the region, among the available correlations. This study follows such recommendation, comparing estimates of compressibility derived from measurement with various suitable correlations on a comparative basis. Error statistics have been used to gauge the goodness of fit, including Mean Square Error, MSE, and Average Absolute Percent Error,

Table 1 Industry correlations of rock compressibility, C_p (in 1/psi) for carbonates. The unit of the estimated rock compressibility (C_p) values by the correlations is 1/psi

Carbonates	(Consolidated)	Author	Equation
		Hall (1953)	$C_r = 1.782 \times 10^{-6} \varphi^{-0.438}$
		Newman (1973)	$C_r = \frac{0.8535}{(1+2.47664 \times 10^6 \varphi)^{0.9299}}$
		Horne (1990)	$C_r = 10^{-6} \exp(4.026 - 23.07 \varphi + 44.28 \varphi^2)$
		Modified Horne (Jalal 2006)	$C_r = 10^{-6} \exp(3.9952 - 33.933 \varphi + 98.04 \varphi^2)$
		Jalal (2006)	$C_r = \frac{10^{-6}}{0.9574+0.35389\varphi^{1.05}}$

AAPE. The best-matching correlation is selected as the one with the lowest error indicator, particularly MSE.

Log-based method

The second approach used in this study to estimate compressibility is the so-called dynamic measurement approach, the use of petrophysical well log data. As well logs, including sonic are acquired under in situ reservoir conditions of stress, essentially uniaxial, log-derived compressibility should be equivalent to uniaxial strain compressibility, which is an advantage (Khatchikian 1995). The log-based method can also offer an option of early pore compressibility estimation for field development without extensive SCAL at high cost (Saxena 2011). Finally, the log-based method has the added benefit of providing a continuous profile of the computed pore compressibility with depth which allows for convenient compaction calculations (Wolfe et al. 2005). Despite all these advantages, dynamic pore compressibility tends to underestimate compressibility due to the existence of microcracks (Geertsma 1957), unless the dynamic effect is considered.

Various studies for the log-based approach have been reported in the literature, but most of these are for sandstones, for example, Ong et al (2001) and Wolfe et al (2005), using a mathematical model comprising computation of rock mechanical properties. There are a few literature references for carbonates, e.g., Saxena (2011), using a differential effective medium (DEM) model, applicable for complex carbonates. However, the methodology applied in the study reported here was not the complex methodology of Saxena but rather similar to that of Ong et al and Wolfe et al., assuming that matrix compressibility can be assumed to be negligible for carbonates. The procedure is outlined below.

After gathering petrophysical well logs and related information: gamma ray, dipole sonic slowness, neutron density, interpreted lithology and porosity, a quality check was executed first. Comparing caliper log readings with hole size, wellbore washouts due to sloughing of the fractured carbonate rocks were identified, with extreme washouts resulting in log readings deemed unreliable. Next, the available laboratory-measured, geomechanical data on cores from this well were collected.

In order to make a valid comparison of compressibility, log-derived with that from core, NOBP values should be evaluated using Eq. 6, which requires vertical, overburden stress, pore pressure and Biot's coefficient. For the logged interval of 8383–9187 ft (2555–2800 m), the vertical stress, σ_v is found using the bulk density log. For the non-logged section, above 8383 ft (2555 m), the overburden pressure gradient of 1.1 psi/ft was chosen, commonly in use for the region. The pore pressure, P_p was obtained from wireline

logs. Biot's coefficient, α was assumed equal to 0.9, to be compatible with the value considered in the core-based method. Having gathered all of the required data, the following procedure was followed to find the estimated log-based pore compressibility:

Log-based procedure

To estimate C_p vs NOBP, a geomechanical earth model (MEM) was essentially constructed, using as input the petrophysical log data and the pore pressure profile. Assuming zero matrix compressibility and the elastic rock, the following five steps were taken to find the pore compressibility for each NOBP:

Estimation of $K_{b,d}$

The bulk modulus represents the effective pressure, NOBP change with respect to the relative bulk volume change, $\frac{\Delta V_b}{V_b}$:

$$K_{b,d} = - \frac{\Delta(\text{NOBP})}{\frac{\Delta V_b}{V_b}} \quad (11)$$

Using the following log parameters: acoustic compressional wave velocity, V_p , shear slowness, V_s , and the density, ρ_b , the dynamic bulk modulus, $K_{b,d}$ was estimated (Gatens et al. 1990; Yu and Smith 2011; Munir et al. 2011):

$$K_{b,d} = \frac{\rho_b}{3} (3V_p^2 - 4V_s^2) \quad (12)$$

Equation 12 may be alternatively written as shown in Eq. 13, using the reciprocal relation of wave velocity and slowness ($V_p = \frac{1}{\Delta t_p}$ and $V_s = \frac{1}{\Delta t_s}$):

$$K_{b,d} = \rho_b \left(\frac{3\Delta t_s^2 - 4\Delta t_p^2}{3\Delta t_s^2 \Delta t_p^2} \right) \quad (13)$$

Conversion of $K_{b,d}$ to $K_{b,s}$

The next step involves the conversion of the dynamic bulk modulus ($K_{b,d}$) to the static one ($K_{b,s}$). Based on Fjaer et al (2008), the bulk modulus is related to Young's modulus, E and Poisson's ratio, ν as follows:

$$K_b = \frac{E}{(1 - \nu)} \quad (14)$$

Writing Eq. 14 both for the static and dynamic cases and taking the ratio gives:

$$\frac{K_{b,s}}{K_{b,d}} = \frac{\frac{E_s}{(1-\nu_s)}}{\frac{E_d}{(1-\nu_d)}} \quad (15)$$

Assuming $\nu_s = \nu_d$ in Eq. 15, appropriate for an elastic medium (Larsen et al. 2000):

$$\frac{K_{b,s}}{K_{b,d}} = \frac{E_s}{E_d} \quad (16)$$

Alternatively:

$$K_{b,s} = K_{b,d} \frac{E_s}{E_d} \quad (17)$$

Some log-based compressibility estimation approaches in the literature have attempted converting the dynamic to static moduli (Khatchikian 1995) by considering only drained conditions, i.e., converting undrained conditions to the drained dry situations using Gassman's equation (Gassmann 1951; Domenico 1977). However, these references are less comprehensive as they do not consider all the reasons for arising discrepancies, as differences between dynamic and static moduli may be attributable to several causes. Discrepancies arise due to different drainage conditions, different strain amplitudes and rates, possible rock heterogeneity and anisotropy (Fjaer 2019). Firstly, comparing drainage conditions gives an indication that deformations induced by elastic dynamic waves in a fully saturated rock are always undrained, while "static" deformations are often drained (Gassmann 1951; Biot 1955). Secondly, different frequency or strain amplitudes need to be considered (Plona and Cook 1995), where strain amplitudes are typically of the order of 10^{-7} for dynamic tests and 10^{-2} to 10^{-3} for static tests. A closed crack or an uncemented grain contact may remain immobilized during the oscillating, low amplitude deformation associated with a passing elastic wave, whereas it may become mobilized as a result of static loading (Walsh 1965). This phenomenon was confirmed by other researchers (Cheng and Johnston 1981; Jizba and Nur 1990; Khatchikian 1995; Fjaer 1999), who found that the difference decreases at high confining stresses, inferring that microcracks close under confining pressures (Geertsma 1957). As an example, Cheng and Johnston (1981) found that the ratio of static to dynamic modulus for some sandstone samples varied from 0.5 at atmospheric conditions to 0.9 at 2800 psi. Based on Eissa and Kazi (1988), the ratio of E_s/E_d usually ranges from 0.5 to 1. As $\frac{E_s}{E_d} < 1$, therefore, $K_{b,s} < K_{b,d}$.

To consider the above issues and possible discrepancies, it is recommended to use core laboratory data to relate the dynamic (log-based) E_d to the static Young's modulus from core, E_s . In this approach, the dynamic and static bulk moduli are also correlated. There are several correlations

between dynamic and static Young's moduli (Elkatatny et al. 2018). The approach followed here was that used by Wang (2000) and Ashena et al. (2020):

$$E_s = 0.4145E_d - 1.0593 \quad (18)$$

Therefore:

$$K_{b,s} = K_{b,d} \left(0.4145 - \frac{1.0593}{E_d} \right) \quad (19)$$

Conversion of $K_{b,s}$ to $C_{b,s}$

Generally, the bulk compressibility coefficient, C_b is defined as the reciprocal of the bulk modulus, K_b . The static bulk compressibility, $C_{b,s}$ can then be expressed as:

$$C_{b,s} = \frac{1}{K_{b,s}} \quad (20)$$

Similarly, $\frac{C_{b,s}}{C_{b,d}} = \frac{K_{b,d}}{K_{b,s}} = \frac{E_d}{E_s}$, and $C_{b,s} > C_{b,d}$.

Conversion of $C_{b,s}$ to C_p

Static bulk compressibility data ($C_{b,s}$) is essentially converted to static pore compressibility ($C_{p,s}$), simply named pore compressibility (C_p). Considering Eq. 10, C_p (or C_r) is found for the log depth interval:

$$C_p = C_r = \frac{C_{b,s}}{\phi} \quad (21)$$

Final calibration

During the process of determining C_p values using petrophysical well logs and static Young's moduli from core data were considered, to find a calibrated correlation for conversion of the dynamic moduli to static ones, Eq. 18. In comparing log and core-derived values for C_p , and in case there is a mismatch between the log-estimated value and the measured value on core, the correlation converting the dynamic to static moduli should be updated until the best match is obtained. Based on the results, if the log-based C_p values are found near the core measurements, this stage may be ignored, as was the case with this case study. It should be noted that some discrepancy between the laboratory results and the log-based compressibility estimates is considered natural due to:

- a possible error in the conversion of the dynamic to static moduli using empirical correlations in the log-based method,

- differences between the hydrostatic nature of experimentally derived compressibility and real anisotropic in situ stress conditions, and
- differences in the fluid type in pores.

Different fluid contained in the core samples (gas, oil or salt water) influence measured pore compressibility. This variation is often ignored by petrophysicists and core lab technicians. Depending on the type of measuring apparatus, the fluid type in the core samples is different:

- In the Core Compressibility Measurement System (CMS), dry (air-bearing) core samples are used, resulting in measured C_r values that are not fully representative of oil-bearing core samples. This situation causes a difference between the core laboratory compressibility measurement and the real one. In this study, laboratory compressibility data were obtained using the CMS apparatus.
- In the Rock Compressibility System (RCS), brine-containing core samples are used. The fluid error is much lower using RCS measurements compared to CMS measurements.

Results

Best-matching correlation

To develop rock compressibility correlations, 45 laboratory-measured compressibility data values were utilized from an Asmari carbonate formation, representative of Southwest Iran. These measurements were plotted on a graph with various industry correlations in the background, Fig. 1. These correlations are: Hall (1953); Newman (1973) and modified Horne (Jalalh 2006). Comparing measurements with each of

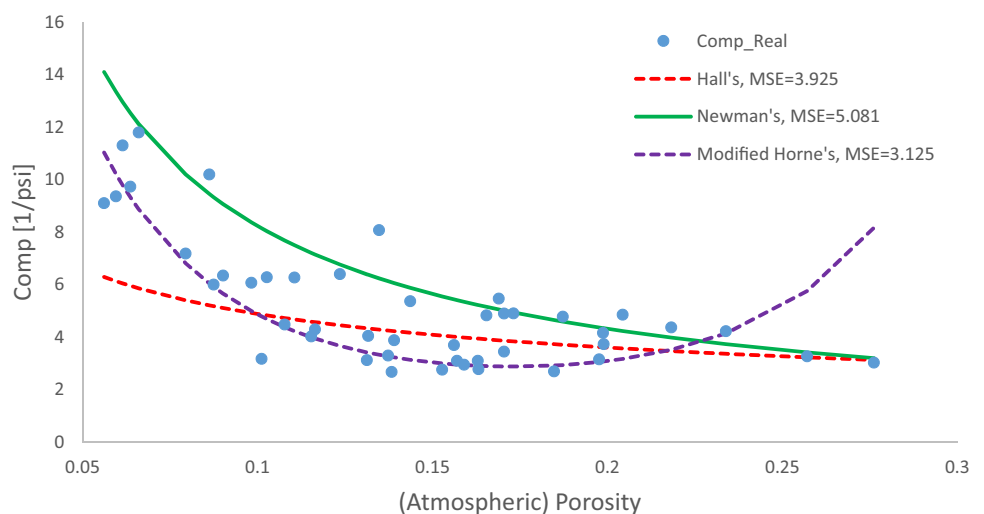
the correlations and using the error metrics described earlier, Table 2 shows that the modified Horne correlation gives the best overall match to the data, with the lowest MSE error of 3.125, the Absolute Root MSE (ARMSE) of 1.767, and an AAPE of 24.44%. Conversely, Newman's equation was identified as the poorest matching correlation. It is, therefore, recommended that the modified Horne correlation should be used to estimate rock compressibility for other Asmari carbonate formations in the region. Equations for error statistics used are listed in "Appendix 1".

Taking a closer look at the distribution of data points in Fig. 1, it can be observed that all correlations converge at higher porosity values where variations in lithology are less sensitive. Conversely, lithology effects tend to be amplified for lower porosity values, particularly in the presence of micro-fractures/ cracks and vugs due to leached marine shell fragments, commonly encountered in Asmari carbonate formations. More elevated compressibility values observed (Fig. 1) at lower porosity values are probably related to the lithology variations mentioned. It should also be mentioned that Newman's correlation was derived for less consolidated carbonates, compared to Hall's correlation, where it can be seen that Newman's correlation is a good representation of the more elevated compressibility values observed for samples from this study.

Table 2 Error statistics, laboratory measurements vs correlations, identifying the Modified Horne correlation (Jalalh 2006) as the best-matching correlation, with the least MSE and ARMSE

	Hall's	Newman's	Modified Horne's
MSE	3.925	5.081	3.125
ARMSE	1.981	2.254	1.767
AAPE [%]	25.568	42.695	24.44

Fig. 1 Core laboratory-derived compressibility values for Iranian, Asmari carbonate, compared with industry, empirical correlations: Hall (1953), Newman (1973) and modified Horne (Jalalh 2006)



Log-based method

Figure 2 shows petrophysical well logs, consisting of gamma ray, dipole sonic slowness, neutron, density, interpreted lithology and porosity for the well under study. Comparing the caliper log readings with the hole size, one can observe the occurrence of wellbore washout due to sloughing of the

fractured carbonate rocks. The adverse effect of washout has been compensated in most intervals, except at some intervals (indicated in the same figure) with extremely high washout. For these intervals, the log readings are deemed to be unreliable.

Figure 3 shows the constructed MEM showing the vertical stress, and current and initial pore pressures (PP and PP_i,

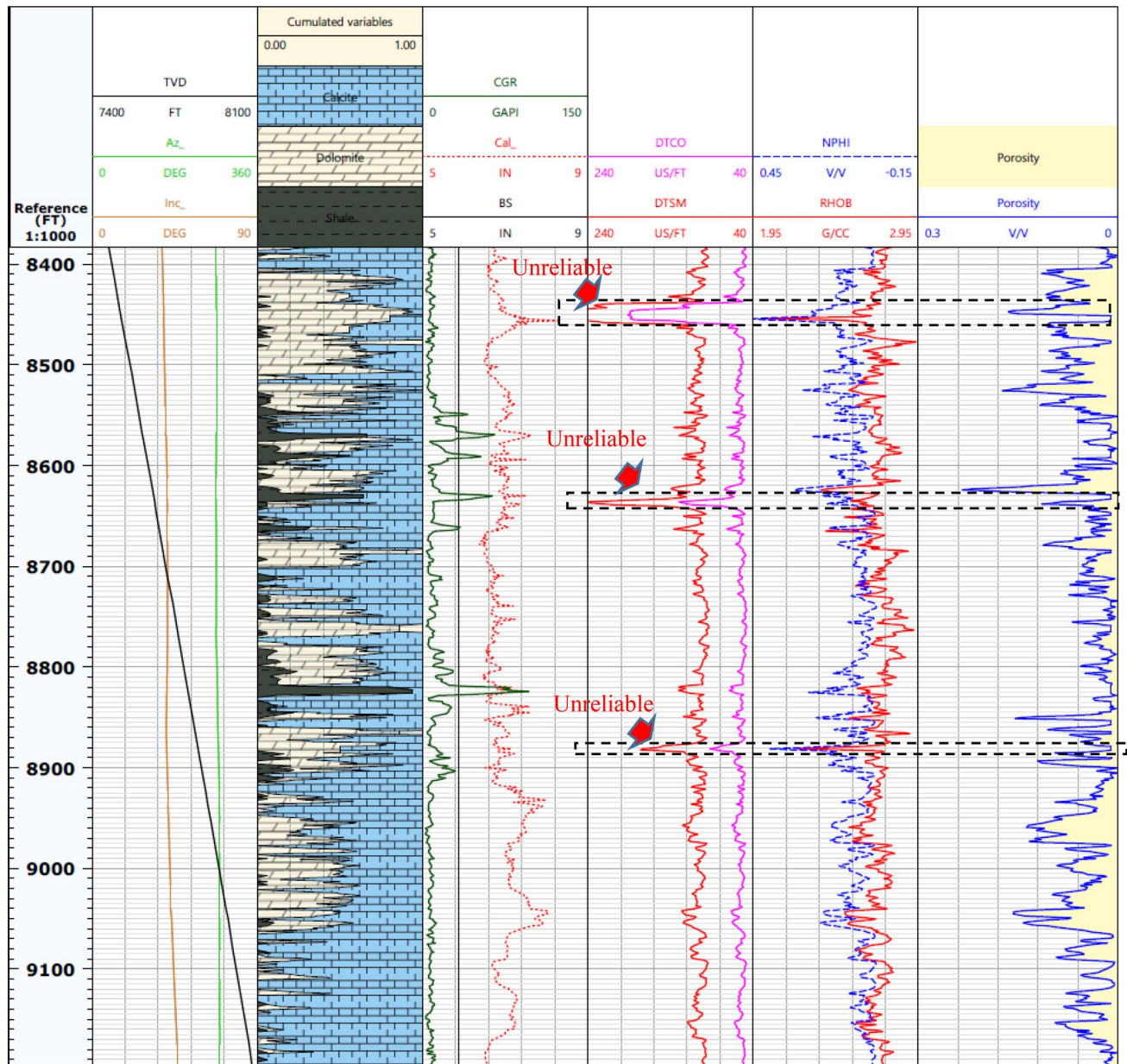


Fig. 2 Petrophysical well logs for the well under study, including interpreted lithology and porosity required for estimation of rock moduli, strength and pore compressibility of the formation for the interval 8383–9187 ft (2555–2800 m). Due to some zones with excessive washout of the wellbore, which can be observed by comparing the caliper and the hole size, log measurements for these zones could not be corrected and are unreliable. Legend: TVD, true verti-

cal depth; Az, azimuth; Inc, inclination angle; DEG, degree; CGR, compensated gamma ray; GAPI, gamma ray unit; Cal, caliper; BS, bit size; IN, inch; DTCO, acoustic compressional slowness; DTSM, acoustic shear slowness; US/FT, micro-second per foot; NPHI, neutron porosity; V/V, (pore) volume to (bulk) volume ratio; RHOB, bulk density, G/CC, gram per cubic centimeter

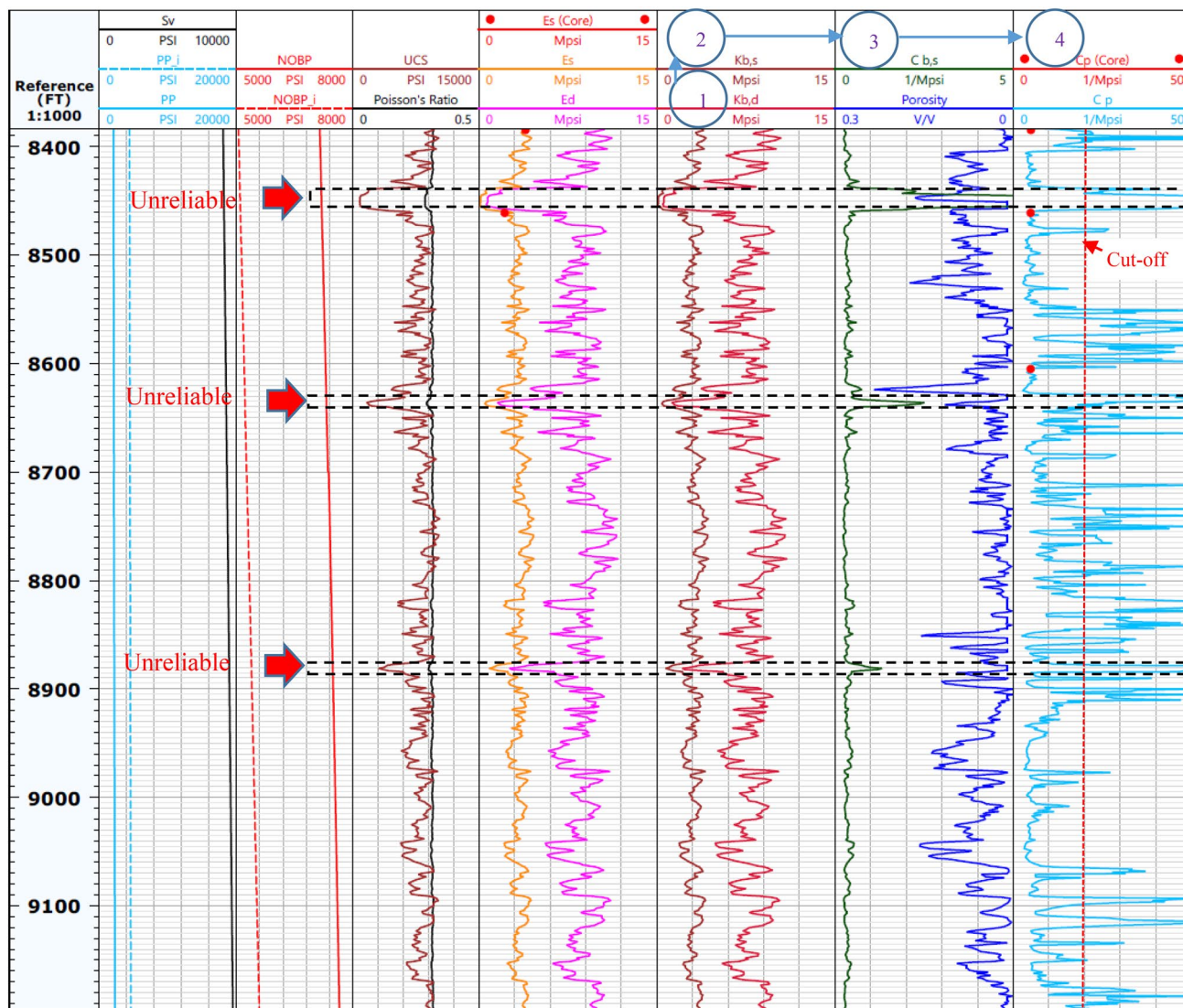


Fig. 3 Geomechanical Earth Model (MEM) constructed for the well under study, including rock moduli, strength and compressibility coefficients for the formation (8383–9187 ft (2555–2800 m)). Four of the pore compressibility evaluation steps are indicated in the figure. Legend: Sv, Vertical Stress; PP_i, initial formation pore pressure; PP, current pore pressure; NOBP, net over-burden pressure; NOBP_i, ini-

tial net over-burden pressure; UCS, uniaxial compressive strength; Ed, dynamic Young’s modulus; Es, static Young’s modulus; Kbd, dynamic bulk modulus; Kbs, static bulk modulus; Cbs, static bulk compressibility; Cp, pore compressibility; Cp (core), pore compressibility (from measured core samples)

respectively), the current and initial NOBP, rock strength (UCS), the dynamic and static Young’s moduli (E_d and E_s from core data), the dynamic and static bulk moduli ($K_{b,d}$ and $K_{b,s}$, respectively), static bulk compressibility ($C_{b,s}$ from core data), porosity and pore compressibility (C_p).

Table 3 shows the available geomechanical laboratory-measured data of core samples for this well under study, which consist of two points for Young’s modulus and three points for core-based pore compressibility. As shown in Table 4, the log-based pore compressibility values show some discrepancy from the core laboratory data: the greatest difference being 58% (absolute percent error, AAPE) at

Table 3 Geomechanical core measurements, including static Young’s modulus and C_p values based on Asmari carbonate, South West Iran

MD (ft)	NOBP (psi)	E_s (Core) (Mpsi)	C_p (Extrapolated from Core) (1/Mpsi)
8384.64	7150	3.95	4.98
8461.15	7200	2.2	4.95
8605.15	7300	–	4.88

the measured depth, MD of 8,384.64 m, with the lowest difference of 19.7% at the MD of 8,461.15 m. As noted above,

Table 4 Log-based compressibility vs core pore compressibility values for Asmari carbonate, Southwest Iran. The core compressibility data is for reliable well log intervals

MD (ft)	NOBP (psi)	$C_{p,l}$ (Log-Based) (1/Mpsi)	$C_{p,c}$ (from Core) (1/Mpsi)	AAPE ($\frac{C_{p,c}-C_{p,l}}{C_{p,c}} \times 100$) (%)
8384.64	7150	7.89	4.98	58.4
8461.15	7200	3.97	4.95	19.7
8605.15	7300	6.37	4.88	30.5

this discrepancy can be attributed to a possible combination of effects: log values due to washouts, the hydrostatic nature of the experimental pore compressibility measurements, the discrepancy in the fluid type, and the possible error in the conversion of the dynamic to static moduli. In layers with unreliable well log measurements, particularly the ones indicated in Figs. 2 or 3, extremely high pore compressibility values are indicated, even greater than 50×10^{-6} /psi, which may be invalid. For layers with extremely low porosity values, in the order of 10^{-4} , typically occurring in thin and tight carbonate layers, extremely high compressibility values can be observed. Considering the possibility of low porosity values in carbonates, a cutoff for pore compressibility may be selected, say $15\text{--}20 \times 10^{-6}$ /psi may be more appropriate, based on this study.

Application to compaction and subsidence

A geomechanical application of compressibility data is the estimation of possible formation compaction and associated subsidence. There are two extreme end-members when considering surface subsidence due to reservoir compaction: (1) plastic flow, the result of competent zones between the reservoir and the surface, and (2) extreme elastic behavior, where there are competent zones present. In the first mentioned case, associated with shallow reservoirs, the surface subsidence bowl is situated directly above the reservoir and its outline mirrors that of the field boundaries below, where the subsidence volume would equate to reservoir voidage using material balance. In the second case, where competent members, e.g., substantial shales are present, the subsidence bowl is aerially significantly larger than the size of the field due to the shales taking up some of the energy through deformation, resulting in a subsidence bowl volume which is significantly less than reservoir voidage.

During hydrocarbon production, the depletion of the reservoir pore pressure leads to significant decrease in the total horizontal stresses (or increase in the effective horizontal stresses), whereas the vertical, overburden stress remains unchanged (Wolfe et al. 2005). Based on the amount of depletion-induced reservoir compaction, adverse effects,

such as subsidence, casing deformation and seismicity may occur. Nagel (2001) gives an overview of compaction and subsidence in the petroleum industry with several field examples.

Many compaction and subsidence studies (e.g. Raghavan et al. 1972; Jelmert and Toverud 2018; Jelmert 2019) are based on certain assumptions to estimate compaction-related subsidence, including constant grain volume, the validity of Darcy's law, instantaneous response to fluid pressure changes, constant overburden stress, and that flow in the vertical direction due to compaction may be neglected. An interesting subsidence study was undertaken for the large Groningen gas field, Netherlands by Hettema et al (2000), utilizing a relatively simple approach to estimating subsidence was applied, relating reduction in reservoir thickness over several decades of production to the subsidence bowl at surface. Considering this approach, an equation can be derived in terms of (absolute) change in reservoir thickness, Eq. 22. For derivation of this equation, see "Appendix 2".

$$|\Delta h| = h_1 \left\{ \frac{\varphi_2}{(\varphi_2 + \exp(C_p \Delta P_p)(1 - \varphi_2))} [1 - \exp(C_p \Delta P_p)] \right\} \quad (22)$$

where φ_2 is the current porosity at the time of the study; $\Delta P_p = P_{p,2} - \Delta P_{p,1}$ (subtraction of the initial pore pressure from the current pore pressure, resulting in negative values).

The above equation for subsidence estimation is comparable with the developed equation by Fjaer et al (2008) assuming linear poroelasticity for a homogenous, isotropic reservoir rock:

$$|\Delta h| = h_1 \times \frac{1}{E_s} \frac{(1 + \nu)(1 - 2\nu)}{(1 - \nu)} \alpha (-\Delta P_p) \quad (23)$$

where E and ΔP_p should be both in the same units, e.g., psi. The negative sign has been used behind ΔP_p to make it positive, and thus, the change in reservoir thickness or ground level is in absolute terms, $|\Delta h|$.

To estimate the change in reservoir thickness with both methods, a stepwise procedure is outlined. Starting with reservoir thickness, h_1 is the difference in true vertical-depth from the mean-sea-level (MSL), TVD_{MSL} (7,471–8,078ft or 2,277–2,462 m), average values for φ_2 and ΔP_p were considered for use in Eq. 22; average values for E_s , ν and α were considered in Eq. 23. The average value for φ_2 was found by taking the average of all log-based porosity values (Fig. 3); the average ΔP_p in the interval was found by subtracting the initial reservoir pressure from the current pore pressure (a negative value); the C_p values were used from the available core laboratory measurements (Tables 3 or 4); the average values for E and ν were found by averaging from Fig. 3, ignoring values for unreliable layers; the average value for α was assumed to be 0.9.

Table 5 summarizes all parameters and also gives the determined subsidence, utilizing both formulations. A surface subsidence of less than 0.4 ft (0.12 m) was estimated to have occurred following 70 years of production history. The reason for this relatively small amount of subsidence, despite an excessive reservoir depletion of 2330 psi, is that the carbonate rock is rather consolidated and the reservoir thickness is just ~600 ft. Recently, using gas injection, the pore pressure has been raised to prevent the continuity of this subsidence phenomenon.

Conclusions

Two methods for obtaining formation compressibility were presented, considering an example for Asmari carbonate formation, Southwest Iran. A comparison was made between laboratory-derived core measurements and values obtained from open-hole logs. These estimates were subsequently used to derive estimates of compaction and related subsidence, based on two alternative formulations.

- To validate laboratory compressibility measurements, it is good practice to compare these against industry correlations. For the Asmari carbonate under study, the modified Horne correlation was found to be the best match to specific laboratory measurements.
- Matching of log-based compressibility with specific core-derived measurements, in this case, Asmari carbonate, is a suitable approach for determining the best overall compressibility for a reservoir. The log-based method utilized was similar to that used for sandstones, following construction of a geomechanical earth model (MEM), resulting in a log of compressibility versus depth. Comparison of the log-based and core data gave a similar result, omitting intervals with large wellbore washout. Some discrepancy was also attributed to the hydrostatic nature of core compressibility measurements. Another reason for some elevated carbonate values observed is related to the diagenetic nature of this, typically micro-fractures and vugs.

Table 5 Parameters for estimation of the subsidence (change of reservoir thickness or ground level) for Asmari carbonate reservoir, refer Eq. 22 (Formulation-1) and Eq. 23 (Formulation-2)

Formulation-1	Formulation-2 (Fjaer et al. 2008)
h_1 [ft] = 607 (185 m)	h_1 [ft] = 607 (185 m)
ΔP_p [psi] = -2330	ΔP_p [psi] = -2330
φ_2 [%] = 4.98	E_s [Mpsi] = 3.5
C_p [1/Mpsi] = 4.9	$\nu = 0.3$
	$\alpha = 0.9$
Δh [ft] = -0.347 (0.082 m)	Δh [ft] = -0.270 (0.082 m)

- The magnitude of possible compaction related subsidence, assuming plastic flow was estimated for a compaction related reservoir thickness change, assuming reservoir depletion resulting in a pressure decrease of 2330 psi, following 70 years of production. An evaluation was performed utilizing two alternative formulations. In this case, due to the competent nature of the carbonate studied, possible subsidence is rather minimal, of the order of 0.4 ft (0.12 m).

Open Access This article is licensed under a Creative Commons Attribution 4.0 International License, which permits use, sharing, adaptation, distribution and reproduction in any medium or format, as long as you give appropriate credit to the original author(s) and the source, provide a link to the Creative Commons licence, and indicate if changes were made. The images or other third party material in this article are included in the article's Creative Commons licence, unless indicated otherwise in a credit line to the material. If material is not included in the article's Creative Commons licence and your intended use is not permitted by statutory regulation or exceeds the permitted use, you will need to obtain permission directly from the copyright holder. To view a copy of this licence, visit <http://creativecommons.org/licenses/by/4.0/>.

Appendix 1: Statistical parameters used for data-fitting

Average absolute percent relative error (AAPE):

$$AAPE = 100 \frac{1}{n} \sum_{i=1}^n \left| \left[\frac{P_m - P_e}{P_m} \right]_i \right| \quad (24)$$

where P_m is the measured parameter; P_e is the evaluated parameter; n is the number of data points.

Mean Square Error or MSE:

$$MSE = \frac{1}{n} \sum_{i=1}^n e_i^2 \quad (25)$$

where:

$$e_i = [P_m - P_e]_i \quad (26)$$

Average Root Mean Square Error (ARMSE):

$$ARMSE = \sqrt{\frac{1}{n} \sum_{i=1}^n e_i^2} \quad (27)$$

Standard Deviation (SD):

$$SD = \left[\frac{n \sum_{i=1}^n E_i^2 - (\sum_{i=1}^n E_i)^2}{n^2} \right]^{\frac{1}{2}} \quad (28)$$

Appendix 2: Derivation of subsidence equation

The derivation is given in three steps, as follows:

Pore volume change

During hydrocarbon production and assuming reservoir pressure depletion, NOBP increases proportionally, where $d\text{NOBP} = -dP_p$. Using this equality and integrating both sides of Eq. 5 for C_p , gives the following for V_p :

$$\int_{P_1}^{P_2} C_p dP_p = \int_{V_{p,1}}^{V_{p,2}} \frac{dV_p}{V_p}$$

$$\ln\left(\frac{V_{p,2}}{V_{p,1}}\right) = C_p \Delta P_p$$

The above equation can be rewritten as:

$$V_{p,2} = V_{p,1} \exp(C_p \Delta P_p) \quad (29)$$

where $\Delta P_p = P_2 - P_1$, which is negative.

Porosity change

To find the change in porosity, Eq. 5 is considered in terms of C_p , where V_p/V_b is replaced by ϕ , and $d\text{NOBP}$ is replaced by $-dP_p$, resulting in:

$$C_p = \frac{1}{V_p} \frac{dV_p}{dP_p} = \frac{1}{V_b} \frac{dV_p}{dP_p} = \frac{1}{\left(\frac{V_p}{V_b}\right)} \frac{d\left(\frac{V_p}{V_b}\right)}{dP_p}$$

Simplifying:

$$C_p = \frac{1}{\phi} \frac{d\phi}{dP_p} \quad (30)$$

Rearranging and integrating Eq. 30 gives the following result:

$$\phi_2 = \phi_1 \exp(C_p \Delta P_p) \quad (31)$$

where $\Delta P_p = P_{p,2} - P_{p,1}$, which is negative.

Alternatively, Eq. 31 can be obtained by dividing both sides of Eq. 29 by the bulk volume, V_b , assuming the volume remains constant during compaction. However, ignoring the bulk volume change resultants in an unacceptable, final porosity, ϕ_2 . To find a more accurate equation for ϕ with respect to pore pressure, a bulk volume change

with pressure is considered. Assuming the matrix volume change to be zero during a pressure change:

$$V_{b,1} - V_{p,1} = V_{b,2} - V_{p,2} \quad (32)$$

Dividing both sides of Eq. 29 by the two sides of Eq. 32 gives:

$$\frac{V_{p,2}}{V_{b,2} - V_{p,2}} = \frac{V_{p,1}}{V_{b,1} - V_{p,1}} \exp(C_p \Delta P_p)$$

Multiplying and dividing both sides of the above equation by the corresponding bulk volumes ($V_{b,2}$ and $V_{b,1}$), gives:

$$\frac{\frac{V_{p,2}}{V_{b,2}}}{\frac{V_{b,2} - V_{p,2}}{V_{b,2}}} = \frac{\frac{V_{p,1}}{V_{b,1}}}{\frac{V_{b,1} - V_{p,1}}{V_{b,1}}} \exp(C_p \Delta P_p)$$

Considering the definition of porosity gives:

$$\frac{\phi_2}{1 - \phi_2} = \frac{\phi_1}{1 - \phi_1} \exp(C_p \Delta P_p) \quad (33)$$

Rearranging gives the final result:

$$\phi_2 = \frac{\exp(C_p \Delta P_p)}{\frac{1}{\phi_1} - [1 - \exp(C_p \Delta P_p)]} \quad (34)$$

Subsidence

To find the equation for subsidence or ground level change, and assuming plastic flow, the ratio of heights (h_2/h_1) is proportional to the ratio of bulk volumes as follows:

$$\frac{h_2}{h_1} = \frac{V_{b,2}}{V_{b,1}} \quad (35)$$

Assuming the matrix volume remains unchanged during compaction, and multiplying and dividing the right hand side of Eq. 35 by the equivalent matrix volumes in Eq. 32 gives:

$$\frac{h_2}{h_1} = \frac{V_{b,2} (V_{b,1} - V_{p,1})}{V_{b,1} (V_{b,2} - V_{p,2})}$$

The right-hand side of the above equation can be rearranged as follows:

$$\frac{h_2}{h_1} = \frac{V_{b,2} (V_{b,1} - V_{p,1})}{V_{b,1} (V_{b,2} - V_{p,2})} = \frac{\frac{(V_{b,1} - V_{p,1})}{V_{b,1}}}{\frac{(V_{b,2} - V_{p,2})}{V_{b,2}}}$$

Simplifying gives:

$$\frac{h_2}{h_1} = \frac{(1 - \varphi_1)}{(1 - \varphi_2)} \quad (36)$$

Combining Eqs. 36 and 33 gives the following:

$$\frac{h_2}{h_1} = \frac{\varphi_1}{\varphi_2} \exp(C_p \Delta P_p) \quad (37)$$

Replacing $\frac{\varphi_1}{\varphi_2}$ in Eq. 37 with its equivalent in Eq. 34 results in the following:

$$\frac{h_2}{h_1} = 1 - \varphi_1 [1 - \exp(C_p \Delta P_p)] \quad (38)$$

Using Eq. 37, the change in reservoir thickness, Δh can be expressed as:

$$\Delta h = h_1 \left[\frac{\varphi_1}{\varphi_2} \exp(C_p \Delta P_p) - 1 \right] \quad (39)$$

And in absolute terms:

$$|\Delta h| = h_1 \left[1 - \frac{\varphi_1}{\varphi_2} \exp(C_p \Delta P_p) \right] \quad (40)$$

Equation 38 can then be rewritten as:

$$|\Delta h| = h_1 \{ \varphi_1 [1 - \exp(C_p \Delta P_p)] \} \quad (41)$$

If the original porosity before any substantial production is not available, φ_1 in Eq. 41 is replaced by its equivalent in terms of φ_2 , taken from Eq. 34, resulting in the alternative expression:

$$|\Delta h| = h_1 \left\{ \frac{\varphi_2}{(\varphi_2 + \exp(C_p \Delta P_p)(1 - \varphi_2))} [1 - \exp(C_p \Delta P_p)] \right\} \quad (42)$$

where φ_2 is the porosity after compaction.

References

- Ashena R, Elmgerbi A, Rasouli V, Ghalambor A, Rabiei M, Bahrami A (2020) Severe wellbore instability in a complex lithology formation necessitating casing while drilling and continuous circulation system. *J Petrol Explor Prod Technol* 10:1511–1532. <https://doi.org/10.1007/s13202-020-00834-3>
- Biot MA (1941) General theory of three-dimensional consolidation. *J Appl Phys* 12:155–164
- Biot MA (1955) Theory of elasticity and consolidation for a porous anisotropic solid. *J Appl Phys* 26:182–185
- Cheng CH, Johnston DH (1981) Dynamic and static moduli. *Geophys Res Lett* 8(1):39–42. <https://doi.org/10.1029/g1008i001p00039>
- Domenico SN (1977) Elastic properties of unconsolidated porous sand reservoirs. *Geophysics* 42(7):1339–1368. <https://doi.org/10.1190/1.1440797>

- Eissa EA, Kazi A (1988) Relation between static and dynamic Young's moduli of rocks. *Int J Rock Mech Min Sci Geomech Abstr* 25:479–482
- Elkatatny S, Mahmoud M, Mohamed I et al (2018) Development of a new correlation to determine the static Young's modulus. *J Petrol Explor Prod Technol* 8:17–30. <https://doi.org/10.1007/s13202-017-0316-4>
- Falcao F, Soares AC, Compan AL, Cruz D, Justen JC, Surmas R, Silveira AJ (2015) A rock mechanics approach for compressibility determination: an important input for petroleum reservoir simulation. In: Rocca RJ et al (eds) *Integrating innovations of rock mechanics*. IOS Press, Amsterdam
- Farsimadan M, Dehghan AN, Khodaei M (2020) Determining the domain of in situ stress around Marun Oil Field's failed wells, SW Iran. *J Petrol Explor Prod Technol* 10:1317–1326. <https://doi.org/10.1007/s13202-020-00835-2>
- Fjær E (1999) Static and dynamic moduli of weak sandstones. In: Ama-dei B, Kranz RL, Scott GA, Smeallie PH (eds) *Rock mechanics for industry*. Balkema, Rotterdam, pp 675–681
- Fjaer E (2019) Relations between static and dynamic moduli of sedimentary rocks. *Geophys Prospect* 67:128–139
- Fjaer E, Holt RM, Horsrud P (2008) *Petroleum related rock mechanics*, 2nd edn. Elsevier Science. ISBN: 9780080557090 (online), ISBN: 9780444502605 (print)
- Gassmann F (1951) Ueber die Elastizitaet poroeserMedien. *Vierteljahrsschrift der Naturforschenden Gesellschaft in Zürich* 96:1–23
- Gatens JM III, Harrison CW III, Lancaster DE, Guidry FK (1990) In-situ stress tests and acoustic logs determine mechanical properties and stress profiles in the Devonian Shales. *SPE 18523, SPE Form. Eval*, pp 248–254
- Geertsma J (1957) The effects of fluid pressure decline on volumetric changes of porous rocks. *Petrol Trans AIME* 210:331–340
- Ghalambor A, Hayatdavoudi A, Koliba R (1994) A study of the sensitivity of relevant parameters to predict sand production. *SPE Paper No. 27011*, proceedings of the 3rd Latin American and Caribbean petroleum engineering conference, V.II, pp. 883–895, 27–29 April 1994, Buenos Aires, Argentina
- Hakiki F, Shidqi M (2018) Revisiting fracture gradient: Comments on “A new approaching method to estimate fracture gradient by correcting Matthew-Kelly and Eaton's stress ratio”. *Petroleum*. <https://doi.org/10.1016/j.petlm.2017.07.001>
- Hall HN (1953) Compressibility of reservoir rocks. *Petrol Trans AIME* 198:309–311
- Hettema MHH, Schutjens PMTM, Verboom BJM, Gussinklo HJ (2000) Production-induced compaction of a sandstone reservoir: the strong influence of stress path. *SPE Reserv Evaluat Eng* 3(4):342–347
- Horne RN (1990) *Modern well test analysis, a computer-aided approach*. Petroway Inc, Palo Alto
- Jalalh AA (2006) Compressibility of porous rocks: part II. New relationship. *Acta Geophysica* 54(4):399–412. <https://doi.org/10.2478/s11600-006-0029-4>
- Jelmert TA (2019) Behavior of compacting reservoirs with restricted entry wells. *J Petrol Explor Prod Technol* 9:3007–3019. <https://doi.org/10.1007/s13202-019-0700-3>
- Jelmert TA, Toverud T (2018) Analytical modeling of sub-surface porous reservoir compaction. *J Pet Explor Prod Technol* 8:1129–1138
- Jizba D, Nur A (1990) Static and dynamic moduli of tight gas sandstones and their relation to formation properties. Presented at SPWLA Annual Logging Symposium
- Khatchikian R (1995) Deriving pore-volume compressibility from well logs. *SPE 26963*, SPE advanced technology series, vol 4, no 1
- Larsen I, Fjaer E, Renlie L (2000) Static and dynamic Poisson's ratio of weak sandstones. In: *ARMA-2000-0077*, 4th North

- American rock mechanics symposium, 31 July–3 August, Seattle, Washington
- Laurent J, Bouteica MJ, Sarda JP, Bary D (1993) Pore pressure influence in the poroelastic behavior of rocks: experimental studies and results. SPE-20922-PA. SPE Formation Evaluation 9:117–122
- Munir K, Iqbal MA, Farid A et al (2011) Mapping the productive sands of Lower Goru Formation by using seismic stratigraphy and rock physical studies in Sawan area, southern Pakistan: a case study. J Petrol Explor Prod Technol 1:33–42. <https://doi.org/10.1007/s13202-011-0003-9>
- Nagel NB (2001) Compaction and subsidence issues within the petroleum industry: from Wilmington to Ekofisk and beyond. Phys Chem Earth (A) 26(1–2):3–14
- Newman GH (1973) Pore volume compressibility of consolidated, friable and consolidated reservoir rocks under hydrostatic loading. J Petrol Technol 25:129–134. <https://doi.org/10.2118/3835-PA>
- Ong S, Zheng Z, Chhajlani R (2001) Pressure-dependent pore volume compressibility—a cost effective log-based approach. SPE 72116, Presented at the SPE Asia Pacific Improved Oil Recovery Conference, K.L., Malaysia, Oct. 8–9
- Plona TJ, Cook JM (1995) Effects of stress cycles on static and dynamic Young's moduli in Castlegate sandstone. In: ARMA-95-0155, Presented at the 35th U.S. Symposium on Rock Mechanics (USRMS), 5–7 June, Reno, Nevada
- Raghavan R, Scorer JDT, Miller FG (1972) An investigation by numerical methods of the effect of pressure-dependent rock and fluid properties on well tests. In: SPE Journal, June, pp 265–275
- Ramiah K, Trivedi KB, Opuwari M (2019) A 2D Geomechanical model of an offshore gas field in the Bredasdorp Basin, South Africa. J Petrol Explor Prod Technol 9:207–222. <https://doi.org/10.1007/s13202-018-0526-4>
- Santamarina J, Park J, Terzariol M et al (2019) Soil properties: Physics inspired, data driven. In: Lu N, Mitchell J (eds) Geotechnical fundamentals for addressing new world challenges. Springer series in geomechanics and geoengineering. Springer, Cham
- Saxena V (2011) A novel technique for log-based pore volume compressibility in complex carbonates through effective aspect ratio. SPE 149124, Presented at the SPE/DGS Saudi Arabia Section Technical Symposium and Exhibition, Al-Khobar, Saudi Arabia, May 15–18
- Terzaghi K (1936) The shearing resistance of saturated soils and the angle between the planes of shear. In: Proceedings of international conference on soil mechanics and foundation engineering, vol 1, pp 54–56. Harvard University Press, Cambridge
- Van der Knaap W (1959) Nonlinear behavior of elastic porous media. Petrol Trans AIME 216:179–187
- Walsh JB (1965) The effect of cracks on the uniaxial compression of rocks. J Geophys Res 70:399–411
- Wang Z (2000) Dynamic vs. static properties of reservoir rocks. In: Wang Z, Nur A (eds) Seismic and acoustic velocities in reservoir rocks. Volume 3: recent developments. Published by SEG
- Wolfe C, Russel C, Luise N, Chhajlani R (2005) Log-based pore volume compressibility prediction—a deepwater GOM case study. SPE 95545, Presented at the SPE Annual Technical Conference and Exhibition, Dallas Texas, Oct. 9–12
- Yu JHY, Smith M (2011) Carbonate reservoir characterization with rock property invasion for edwards reef complex. Presented at the 73rd EAGE conference and exhibition incorporating SPE Europe, Vienna, Austria, May 23–26
- Zimmerman RW, Somerton WH, King MS (1986) Compressibility of porous rocks. J Geophys Res 91(B12):12765–12777

Publisher's Note Springer Nature remains neutral with regard to jurisdictional claims in published maps and institutional affiliations.